Enzymic Dynamics and Molecular Orbital Study on the Roles of Arginines in Carboxypeptidase A, a Sliding Mechanism[1]

Setsuko Nakagawa and Hideaki Umeyama*

Contribution from the School of Pharmaceutical Sciences, Kitasato University, Shirokane, Minato-ku, Tokyo, Japan 108. Received April 24, 1978

Abstract: The guanidyl group of arginine is significant as a binding site of anionic substrates or coenzymes. Carboxypeptidase A (CPA) includes arginine residues in its binding groove. X-ray diffraction analyses of CPA showed that Arg-145 acts as a final binding site of the C-terminal carboxylate group of substrates and that Arg-127 and Arg-71 may act as initial binding sites. Since X-ray study is unable to detect dynamic aspects of the enzymatic reaction, the dynamic study of CPA using the molecular orbital method was carried out to study the mechanism of the insertion of substrates into the active site. The study showed that the C-terminal carboxylate of substrates "slides" smoothly to the final binding site of Arg-145 through the initial binding sites of Arg-71 and Arg-127. The scheme of the binding of substrates to Arg-71 and Arg-127 may be described as a "bridge model" on an ion-pair structure. When C-terminal carboxylate reaches the final binding site of Arg-145, Arg-71 and Arg-127 bind with two carbonyl oxygens of the substrate. The product of the hydrolyzed substrate may leave easily from the active site by changing the structure from $-NH-$ to $-NH_3^+$. Moreover, the ab initio calculation was done for the complexes between guanidinium ion and formic acid ion, formamide, or glycine ($NH_3^+CH_2COO^-$ or $NH_2CH_2COO^-$), and the origin of those complexes was elucidated by energy decomposition and charge-distribution analyses.

Introduction

Many enzymes contain arginyl residue at their active site and in such cases enzymatic activities are reduced by chemical modification of the residues.[2] Arginyl residue exhibits a high pK_a and is positively charged in aqueous solution. The residues can serve as a positively charged recognition site for negatively charged substrate or anionic coenzyme in the active site of enzymes. For instance, guanidinium ions of Arg-35 and Arg-87 of staphylococcal nuclease form two hydrogen bonds with the 5′-phosphate of the inhibitor.[3] In the active site of the abortive lactate dehydrogenase–nicotinamide adenine dinucleotide-pyruvate ternary complex, Arg-101 forms two hydrogen bonds with the pyrophosphate of coenzyme, and Arg-171 forms hydrogen bonds with the carboxyl group of the substrate.[4] In the active site of carboxypeptidase A (CPA), when the C-terminal side chain of the substrate is inserted into the pocket, the guanidyl group of Arg-145 moves 2 Å from the initial position by rotation around the $C^\beta-C^\gamma$ bond of the residue.[5] Arg-145 forms a salt link with the C-terminal carboxylate of the substrate. Then residues of Arg-71, Arg-127, Tyr-198, and Phe-279 may serve as an initial recognition site in the early stage of substrate binding.[5] It seems significant, therefore, to clarify the roles of arginine residues in various enzymes. In this paper the roles of the three arginine residues (Arg-71, Arg-127, and Arg-145) of CPA are studied.

Reaction mechanisms for various enzymes have been clarified by the molecular orbital methods in recent years. α-Chymotrypsin,[6] papain,[7] and lactate dehydrogenase[8] have been investigated with respect to proton transfer in the active site. For CPA, the scissile peptide C–N bond of substrates is weakened by the polarizing effect of the zinc ion.[9] The effect on the energies of distortion of the substrate before the transition state is investigated.[10] The lowering of the transition energy is attributed to the enhanced stability of an sp^3 vs. sp^2 nitrogen. Recently Scheiner and Lipscomb reported by the ab initio MO study of CPA that Zn^{2+} and its ligands are more effective than various hydrogen-bonding species in catalyzing the hydrolysis.[9b] Our efforts were concentrated to elucidate the binding process of a substrate, because many biochemists are very interested in the reason why CPA hydrolyzes the substrate from the C-terminal amino acid. The present paper treats the mechanism of the insertion of substrates into the

active site of CPA by referring to functions of the three arginine residues.

Methods and Geometries. All the calculations have been carried out within the closed shell LCAO (linear combination of atomic orbitals)–SCF (self-consistent field) approximation with the CNDO/2[11] and ab initio methods. Calculations were carried out using HITAC 8700 and 8800 computers in the Tokyo University Computer Center. The GAUSSIAN 70 program[12] was used for ab initio calculations. The basis set for ab initio calculations is STO-3G. The ORTEP program by C. Johnson was used for the drawing of the molecular structures.[13] The total energy was employed to check the convergence in the iteration process. Stabilization energy ($\Delta E = E_{complex} - E_{monomers}$) was decomposed into five components

$$\Delta E = ES + EX + PL + CT + MIX$$

where ES, EX, PL, CT, and MIX are electrostatic, exchange repulsion, polarization, charge transfer, and mixing (= coupling) energies. In ab initio calculations the charge-distribution decomposition analysis was also applied[14]

$$\Delta\rho(r) = \rho_{PL}(r) + \rho_{EX}(r) + \rho_{CT}(r) + \rho_{MIX}(r)$$

where $\rho_{PL}(r)$ is population change by PL term, $\rho_{EX}(r)$ by EX, $\rho_{CT}(r)$ by CT, and $\rho_{MIX}(r)$ by MIX. The definitions of energy- and charge-distribution components and details of the calculation were reported.[15] MIX was decomposed by the method of Nagase et al.[16]

$$\sum_i COP_i = COP_1 + COP_2 + COP_3 + COP_4$$

where COP_1 is the coupling term among occupied and unoccupied MO sets of molecule A and the occupied MO set of B (A_{occ}, A_{vac}, and B_{occ}), COP_2 among A_{occ}, B_{occ}, and B_{vac}, COP_3 among A_{occ}, A_{vac}, and B_{vac}, and COP_4 among A_{vac}, B_{occ}, and B_{vac}.

Geometries of monomers are shown in Figure 1. The geometries of guanidinium ion and formic acid ion in place of the arginine residue and the C-terminal carboxylate are from calculations of Umeyama and Matsuzaki.[17] Formamide is from the book by Sutton.[18] In the glycine zwitterion ($NH_3^+CH_2COO^-$), a moiety, $>CCH_2NH_3^+$, is from a neutron study;[19] $-COO^-$ is from $HCOO^-$. In the glycine anion
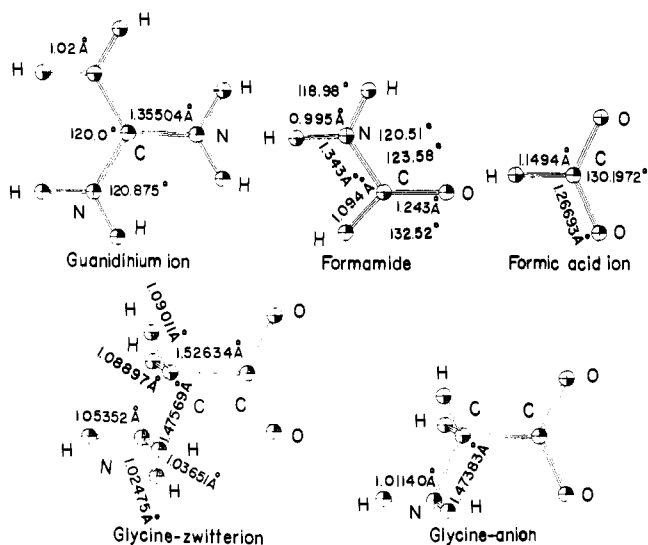
Figure 1. Monomer geometries used in calculations of $C(NH_2)_3^+$, $HCOO^-$, $HCONH_2$, $NH_3^+CH_2COO^-$, and $NH_2CH_2COO^-$.

Figure 3. Complexes between guanidinium ion and glycine zwitterion or glycine anion.

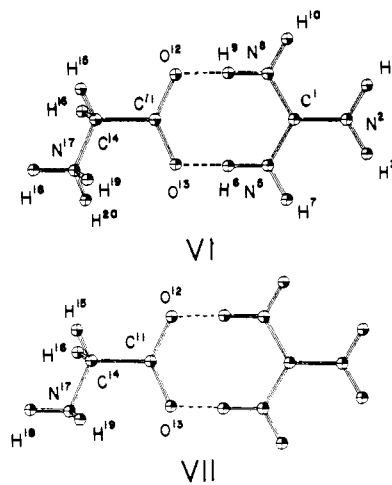**Figure 2.** Various complexes between guanidinium ion and formic acid ion.
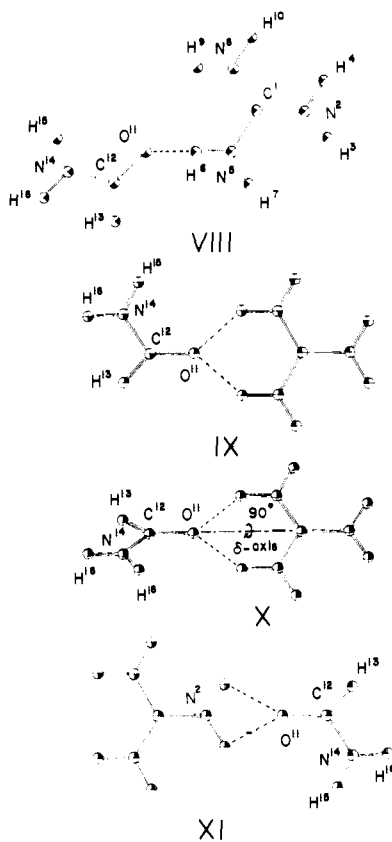
Figure 4. Various complexes between guanidinium ion and formamide.

$(NH_2CH_2COO^-)$, part of the $>CNH_2$ group is from NH_2CH_3;[20] $-COO^-$ is from $HCOO^-$; $>CCH_2-$ is from a neutron study of glycine.[19]

Figure 2 shows the five ion-pair structures between guanidinium ion and formic acid ion. Structure I has two nearly parallel hydrogen bonds. In structure II, formic acid ion rotates around the $O^{12}-O^{13}$ line (α axis) by 30°. In structure III, it rotates around the line parallel to the x axis through the position of O^{13} (β axis) by 30°. Structure IV has only one hydrogen bond which is nearly linear between N^5 and O^{12}. In structure V, it rotates around the C^1-C^{11} line (γ axis) by 90°. VI and VII in Figure 3 show the interacting structures between glycine anion and guanidinium ion and between glycine zwitterion and guanidinium ion, respectively. Figure 4 shows the four interacting structures between guanidinium ion and formamide. Structure VIII has a linear hydrogen bond between N^5 and O^{11}. Structures IX and X have bifurcating hydrogen bonds. In the latter structure, X, formamide rotates around the C^1-C^{11} line (δ axis) by 90°. In structure XI, carbonyl oxygen interacts with an amino group of guanidinium ion and forms bifurcating hydrogen bonds.

The coordinates for the CPA and Gly-Tyr are from the work of Quiocho and Lipscomb.[5c] When the C-terminal of the substrate is inserted into the active site, the C-terminal carboxyl group may slide on three arginine residues. Three guanidinium ions and formic acid ion in Figure 1 were positioned at the site of Arg-71, Arg-127, and Arg-145 of CPA and the C-terminal of Gly-Tyr, respectively.

The C-terminal of Gly-Tyr, Arg-145, and 14 amino acid residues in CPA which were in the neighborhood of Arg-145 were replaced with simple models summarized in Table I. The coordinates of hydrogen atoms were determined as follows. The C-H bond is 1.09 Å and angle $\angle XCH$ is 109.5° in $-CH_3$ and $>CH_2$ groups. In $-NH_2$ and $>NH$ groups, N-H bond is 1.02 Å and angle $\angle XNH$ is 120°. The O-H bond is 0.956 Å and
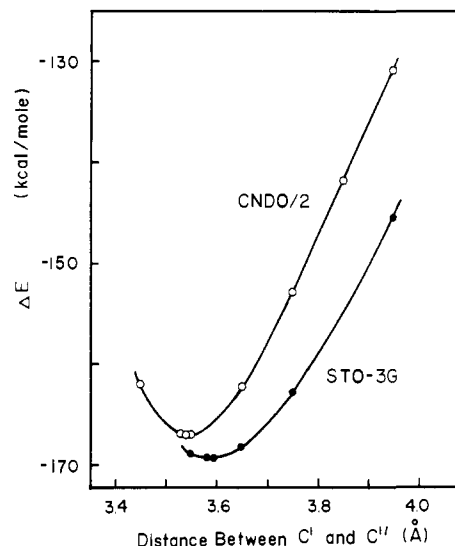
Figure 5. Total interaction energies between guanidinium ion and formic acid ion for various intermolecular distances in structure 1 by using ab initio and CNDO/2 methods. Distances between both carbons of two molecules are used.

Figure 6. Molecular orbital levels of various molecules obtained from ab initio calculations using the STO-3G basis set: A, guanidinium ion; B^1, formic acid ion; B^2, glycine anion; and B^3, glycine zwitterion. Numbers of π MO's are 14, 15, 16, and 17 for A; 8, 12, and 13 for B^1; 15, 20, and 21 for B^2; and 16, 20, and 22 for B^3.

Table I. Structures Used in Calculations in Place of Various Amino Acid Residues and the Backbones

residues and backbones	calcd molecules
Arg-71	$C(NH_2)_3^+$
Arg-127	$C(NH_2)_3^+$
Asp-142	CH_3COO^-
Asn-144	CH_3CONH_2
Arg-145	$CH_3CH_2NHC(NH_2)_2^+$
Glu-163	$CH_3CH_2COO^-$
Thr-164	CH_3CHCH_3OH
Tyr-248	C_6H_5OH
Asp-256	CH_3COO^-
Asn-144–Arg-145	CH_3CONH_2
Gly-155–Ala-156	CH_3CONH_2
Tyr-248–Gln-249	CH_3CONH_2
Gln-249–Ala-250	CH_3CONH_2
Ala-250–Ser-251	$CH_3CH_2CONH_2$
Gly-252–Gly-253	$HCONHCH_3$
Gly–Tyr(C-terminal)	CH_3COO^-

angle $\angle$XOH is 108.9°. Since Lipscomb et al. did not report the coordinates of Arg-145 interacting with $-COO^-$ of the C-terminal of the substrate,[21] these coordinates were obtained by applying the rotations of -40, 40, and 20° to the clockwise direction around the bonds $C^\beta-C^\gamma$, $C^\gamma-C^\delta$, and $C^\delta-N^\epsilon$, respectively. The movement of Arg-145 was 2.45 Å for the carbon in the guanidyl group. The movement of Tyr-248 by the rotation of -120, -150, -60, and 30° around the bonds C^O-C^α, $C^\alpha-C^\beta$, $C^\beta-C^\gamma$, and $C^\zeta-C^\eta$, respectively, induces the following movements: for Ala-250, 20 and $-20°$ rotation around C^O-C^α and $C^\alpha-N$; for Gln-249, 80° rotation around $C^\alpha-N$. After the movement of 12.73 Å of hydroxyl oxygen in Tyr-248, the distance between the hydroxyl oxygen and the susceptible nitrogen in Gly-Tyr is 2.75 Å.

Complex between Guanidinium Ion and Formic Acid Ion. The C-terminal carboxylate of a substrate forms a salt link with the guanidyl group of Arg-145 in the active site of CPA. By using a guanidinium ion and a formic acid ion in place of Arg-145 and the C-terminal carboxylate, interaction energies for various structures were calculated. Those structures were shown in Figure 2. Structure I is an ion pair involving two nearly parallel hydrogen bonds between nitrogen in the gua-
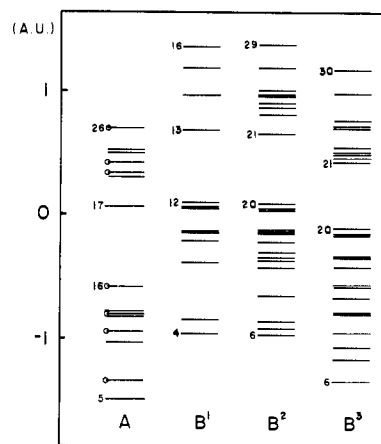
nidinium ion and oxygen in the formic acid ion. The potential curve of this complex is plotted against the distance between both carbons in Figure 5. In STO-3G calculations the most stable state was at the distance of 3.59 Å. Since the CNDO/2 method is used to calculate large molecules, a potential curve was also plotted by the CNDO/2 calculations. The most stable distance was calculated as 3.54 Å, differing from the result of STO-3G calculation by only 0.04 Å. Thus, the potential curves are very similar to each other, and the results obtained by the CNDO/2 method for ion pairs are reliable to discuss.

The energy-decomposition analysis of the above result is shown in Table II. The stabilization energy was 169 kcal/mol at the most stable distance. Electrostatic interaction is the largest (60%).[22] Since net charges of H in the guanidinium ion and O in the formic acid ion are $+0.275$ and -0.515, respectively, the large contribution of ES is explained by the population change of those atoms. Then the contribution of the CT term of 27% for the stabilization is secondly large.[23] Moreover, the CT term is separated into two terms of $CT_{A\rightarrow B}$ and $CT_{B\rightarrow A}$ where $CT_{A\rightarrow B}$ means charge transfer from molecule A to B. The charge-transfer energy from $HCOO^-$ (B) to $C(NH_2)_3^+$ (A) is 71.9 kcal/mol, which is 99.4% of the charge-tranfer energy. Accordingly, the interaction between the unoccupied MO set in $C(NH_2)_3^+$ and the occupied MO set in $HCOO^-$ is significant.

Figure 6 shows molecular orbital levels of $C(NH_2)_3^+$ and $HCOO^-$. Four MO's in $C(NH_2)_3^+$ and three in $HCOO^-$ having large atomic orbital (AO) coefficients in 1s AO's were not shown in this figure. The results of MO interactions between $C(NH_2)_3^+_{vac}$ and $HCOO^-_{occ}$ for structure I are shown in Table III. The MO interaction energy between both σ MO sets of $C(NH_2)_3^+_{vac}$ and $HCOO^-_{occ}$ was 71.8 kcal/mol, which is almost equal to the charge-transfer energy, 71.9 kcal/mol, from $HCOO^-$ to $C(NH_2)_3^+$. On the contrary, the interaction energy between π MO sets of $C(NH_2)_3^+_{vac}$ and $HCOO^-_{occ}$ was almost zero. Since the interaction energy between σ MO sets was significant, further analyses were carried out on those MO's. Firstly, in order to elucidate contribution of occupied MO's in $HCOO^-$, the number of included σ MO's was decreased. When four MO's from the highest occupied MO (HOMO) in $HCOO^-$ interacted with the vacant σ MO set in $C(NH_2)_3^+$, the CT energy was -89.1 kcal/mol, which is more stable than the value of -71.9 kcal/mol of CT_{B-A}. Inclusion of three occupied σ MO's from HOMO gave a similar result to that described above. Since the interaction does not include the lower three σ MO's in the valence state of $HCOO^-$, the

Table II. Total Interaction Energies and Decomposition Analyses for Various Ion-Pair Structures between Guanidinium Ion and Formic Acid Ion in kcal/mol (STO-3G Basis Set)

term	structure I	term Δ	II	III	IV	V
ΔE	−169.4	$\Delta\Delta E$	3.5	20.3	31.4	58.8
ES	−158.5 (60%)	ΔES	2.9	25.4	29.3	54.3
EX	96.7	ΔEX	1.2	−38.3	−28.6	−84.4
PL	−7.4 (3%)	ΔPL	−0.0	1.2	0.5	3.2
CT	−72.4 (27%)	ΔCT	−0.2	22.1	33.1	59.5
MIX	−27.7 (10%)	ΔMIX	2.0	9.9	−2.9	26.3
$CT_{A\rightarrow B}$[a]	−0.4	$\Delta CT_{A\rightarrow B}$	−0.6	0.1	0.1	
$CT_{B\rightarrow A}$	−71.9 (99.4%)	$\Delta CT_{B\rightarrow A}$	0.6	22.0	33.0	59.0
ΣCOP[b]	−26.8	$\Delta\Sigma$COP	2.6	9.8	3.1	
COP_1	−25.1 (92%)	ΔCOP_1	1.5	10.0	5.3	
COP_2	0.6	ΔCOP_2	1.0	−0.6	−0.3	
COP_3	−0.0	ΔCOP_3	0.0	0.0	−0.0	
COP_4	−2.2 (8%)	ΔCOP_4	0.1	0.3	−1.9	

[a] A and B are guanidinium ion and formic acid ion, respectively. [b] Definition of COP_i is shown in Methods and Geometries.

Table III. Molecular Orbital Interaction Energies between Unoccupied MO's in $C(NH_2)_3{}^+$ and Occupied MO's in $HCOO^-$ for Structure I (STO-3G Basis Set)

A_{vac}	σ_{all}	π_{all}	σ_{all}	σ_{all}	σ_{all}	$\sigma_{d\text{-}A}$
B_{occ}	σ_{all}	π_{all}	$\sigma_{a\text{-}B}$	$\sigma_{b\text{-}B}$	$\sigma_{c\text{-}B}$	$\sigma_{d\text{-}B}$
kcal/mol	−71.8	−0.0	−89.1	−88.1	−69.4	−67.6
A_{vac}	$\sigma_{e\text{-}A}$	$\sigma_{f\text{-}A}$	$\sigma_{g\text{-}A}$	$\sigma_{h\text{-}A}$	$\sigma_{i\text{-}A}$	$\sigma_{j\text{-}A}$
B_{occ}	$\sigma_{e\text{-}B}$	$\sigma_{f\text{-}B}$	$\sigma_{g\text{-}B}$	$\sigma_{h\text{-}B}$	$\sigma_{i\text{-}B}$	$\sigma_{j\text{-}B}$
kcal/mol	−65.6	−58.0	−32.2	−18.9	−20.6	−18.9

a-B: 7,[a] 9, 10, 11. b-B: 9, 10, 11. c-B: 10, 11
d-A: 18, 19, 20, 21, 22, 23, 24, 25. d-B: 10, 11
e-A: 18, 19, 20, 21, 22, 23, 24. e-B: 10, 11
f-A: 18, 19, 20, 21, 22. f-B: 10, 11]
g-A: 18, 19, 20. g-B: 10, 11
h-A: 18. h-B: 10, 11]
i-A: 18, 19, 20. i-B: 11]
j-A: 18 (LUMO in σ's). j-B: 11 (HOMO in σ's)]

[a] The meaning of MO level number is shown in Figure 6.

Table IV. Atomic Orbital Coefficients of H^6 and H^9 in the Guanidinium Ion and O^{12} and O^{13} in the Formic Acid Ion for MO Levels Shown in Figure 6

guanidinium ion			formic acid ion		
MO levels	1s of H^6	1s of H^9	MO levels	$2p_x$ of O^{12}	$2p_x$ of O^{13}
17 (π)	−0.000	+0.000	1	+0.001	+0.001
18	+0.442	+0.442	2	+0.002	−0.002
19	−0.167	−0.167	3	−0.001	−0.001
20	−0.593	+0.593	4	+0.041	+0.041
21	+0.631	+0.631	5	−0.044	+0.044
22	+0.287	−0.287	6	−0.166	−0.166
23	−0.227	−0.227	7	−0.096	−0.096
24	−0.521	+0.521	8 (π)	+0.000	−0.000
25	−0.356	+0.356	9	+0.370	−0.370
26	+0.252	+0.252	10	+0.518	−0.518
			11	−0.644	−0.644
			12 (π)	−0.000	−0.000

Table V. Exchange Repulsion Energy Obtained from Intermolecular Overlaps of Occupied Molecular Orbitals in kcal/mol (STO-3G Basis Set)

A_{occ}[a]	MO_{all}[b]	σ_{all}	π_{all}	$\sigma_{11,12,13}$
B_{occ}	MO_{all}	σ_{all}	π_{all}	$\sigma_{10,11}$
kcal/mol	183.4	176.0	0.3	37.2

[a] A and B are the guanidinium ion and formic acid ion, respectively. [b] The number of MO levels is shown in Figure 6.

interaction energy would have been greatly stabilized. That is, the increase of population by CT from the lower three σ MO's to $C(NH_2)_3{}^+{}_{vac}$ may interfere with the charge transfer from the higher four σ MO's to $C(NH_2)_3{}^+{}_{vac}$. The CT interaction energy obtained from inclusion of HOMO and a MO under HOMO in the σ set was −69.4 kcal/mol. The MO under HOMO and HOMO was significant. Table IV shows AO coefficients of two hydrogens of $C(NH_2)_3{}^+$ and two oxygens of $HCOO^-$ being able to interact with each other. The large AO coefficients of HOMO and the MO under the HOMO explain the contribution of those MO's. Next, the number of the vacant MO's in $C(NH_2)_3{}^+$ was decreased. As the number decreases, CT interaction energy decreases. In order to study contributions of HOMO and LUMO, CT energies obtained from MO selections described by σ_g, σ_h, σ_i, and σ_j were compared. The small difference between i and j selections shows the small interaction energy among σ_{19} (over LUMO in σ MO's), σ_{20} in $C(NH_2)_3{}^+$, and σ_{11} (HOMO in σ MO's) in $HCOO^-$. The difference, 13.3 kcal/mol, between g and h selections is due to the interaction among σ_{19}, σ_{20} in $C(NH_2)_3{}^+$, and σ_{10} (under HOMO) in $HCOO^-$. As shown in Table IV signs of the AO coefficients of two oxygens in σ_{10} of $HCOO^-$ are different, but those of σ_{11} are the same. On the other hand, those of two hydrogens of σ_{18} and σ_{19} in $C(NH_2)_3{}^+$ are the same, but those of σ_{20} are different. From the relationships of symmetry, therefore, the interaction energies between σ_{11} and σ_{18} or σ_{19} and between σ_{10} and σ_{20} will be large, but those between σ_{11} and σ_{20} and between σ_{10} and σ_{18} or σ_{19} will be almost

zero. Accordingly the charge transfer from the occupied σ MO set in $HCOO^-$ to the unoccupied σ MO set in $C(NH_2)_3{}^+$ is dominantly affected by many unoccupied MO's in $C(NH_2)_3{}^+$ and many valence occupied MO's in $HCOO^-$.

In structure I exchange repulsion (EX) consists of an intermolecular exchange term ($-\Sigma_i^{Aocc}\Sigma_j^{Bocc}K_{ij}{}^0$) and the exchange repulsion term (EX′) from intermolecular overlap integrals of occupied MO sets. The former term, X, is obtained from ESX-EX in ref 24. Therefore EX is equal to X + EX′. Table V shows the results of EX′. The repulsive energy, EX′, between the occupied MO set in $C(NH_2)_3{}^+$ and the occupied MO set in $HCOO^-$ was 183.4 kcal/mol. Exchange repulsion energy between σ MO sets of both molecules was 176.0 kcal/mol and it explains 96% of the total repulsion energy. Contribution of the π MO set was very small. In order to elucidate the contribution of the neighboring MO's of HOMO, the following MO's were selected: HOMO and two MO's under HOMO in the σ set of $C(NH_2)_3{}^+$ and single MO under

Table VI. Total Atomic Population Changes of Various Complexes between Guanidinium Ion and Formic Acid Ion and Charge-Distribution Decomposition Analysis for Structure I in STO-3G Basis Set

	$\rho(r)_{monomer}$	I $\Delta\rho(r)$	$\rho_{EX}(r)$	$\rho_{PL}(r)$	$\rho_{CT}(r)$	$\rho_{MIX}(r)$	II, $\Delta\rho(r)$	III, $\Delta\rho(r)$	IV, $\Delta\rho(r)$
C^1	5.498	0.056	0.002	0.017	0.004	0.033	0.056	0.040	0.043
N^2	7.385	0.028	0.001	0.018	0.002	0.008	0.028	0.024	0.023
H^3	0.725	0.047	0.000	0.028	0.000	0.018	0.046	0.037	0.031
H^4	0.725	0.047	0.000	0.028	0.000	0.018	0.046	0.042	0.045
N^5	7.385	0.069	0.034	-0.002	-0.002	0.040	0.067	0.055	0.047
H^6	0.725	-0.041	-0.037	-0.080	0.160	-0.085	-0.039	-0.045	-0.048
H^7	0.725	0.081	0.001	0.037	0.002	0.041	0.079	0.073	0.063
N^8	7.385	0.069	0.034	-0.002	-0.002	0.040	0.067	0.027	0.020
H^9	0.725	-0.041	-0.037	-0.080	0.160	-0.085	-0.039	-0.026	-0.002
H^{10}	0.725	0.081	0.001	0.037	0.002	0.041	0.079	0.054	0.046
total		0.397	0.000	0.000	0.326	0.071	0.391	0.282	0.268
C^{11}	5.843	-0.091	0.001	-0.023	-0.014	-0.054	-0.090	-0.056	-0.051
O^{12}	8.515	-0.092	-0.001	0.044	-0.150	0.015	-0.091	-0.072	-0.029
O^{13}	8.515	-0.092	-0.001	0.044	-0.150	0.015	-0.091	-0.057	-0.101
H^{14}	1.127	-0.123	0.001	-0.065	-0.012	-0.046	-0.118	-0.097	-0.087
total		-0.397	0.000	0.000	-0.326	-0.071	-0.391	-0.282	-0.268

HOMO and HOMO in the σ set of $HCOO^-$. The repulsion energy was 37.2 kcal/mol. This value is only 20% of the total repulsion energy. Therefore, the interactions among all the σ MO's of both molecules must be included to calculate the repulsion energy.

The contribution of the mixing term for the stabilization energy was 10% in Table II. The coupling energy was decomposed into four terms. The summation of four coupling terms is shown by ΣCOP. A coupling term, COP_1, which is the interaction among $HCOO^-_{occ}$, $C(NH_2)_3^+_{occ}$ and $C(NH_2)_3^+_{vac}$ is the main contributor.

Table VI shows electron density decomposition for structure I. When the ionic interaction occurs, the total electron density of guanidinium ion increases to the summation value of $\rho_{CT}(r)$ = 0.326 and $\rho_{MIX}(r)$ = 0.071. After the formation of the ion pair, however, H^6 and H^9 which are directly interacting with $HCOO^-$ become electron deficient by 0.041. The decrease of electron density is due to $\rho_{PL}(r)$, $\rho_{EX}(r)$, and $\rho_{MIX}(r)$. Those three density terms cancel the increased value, 0.160, by $\rho_{CT}(r)$. Then the other atoms except for H^6 and H^9 in the electron-acceptor molecule become electron-rich as shown by the increase of $\Delta\rho(r)$ values. The increase in N^5 is due to $\rho_{EX}(r)$ and $\rho_{MIX}(r)$, and C^1, H^3, and H^4 are increased by $\rho_{PL}(r)$ and $\rho_{MIX}(r)$. On the other hand, the electron density in $HCOO^-$ which is the electron-donor molecule decreases to the summation value, 0.397, of $\Delta\rho_{CT}(r)$ and $\Delta\rho_{MIX}(r)$. All the atoms of $HCOO^-$ become electron deficient after the complex formation. Especially the deficiency is large for H^{14}, though it is thought that the electron densities in O^{12} or O^{13} may be largely affected by the interaction. The electron density in O^{12} decreases by 0.092, since $\rho_{CT}(r)$ which is the main contributor is canceled by $\rho_{PL}(r)$. Those of C^{11} and H^{14} decrease due to $\rho_{PL}(r)$, $\rho_{CT}(r)$, and $\rho_{MIX}(r)$.

In structure II $HCOO^-$ is rotated by 30° around the O^{12}–O^{13} line (α axis). The difference in the stabilization energy from structure I is 3.5 kcal/mol. The unstabilization is attributed to ES, MIX, and EX as shown in Table II. ES is the main contributor. EX is increased by the proximity of atoms in both molecules. MIX occurs from the MO interaction among $HCOO^-_{occ}$, $C(NH_2)_3^+_{occ}$, and $C(NH_2)_3^+_{vac}$. Though the CT term from $HCOO^-$ to $C(NH_2)_3^+$ decreases by 0.6 kcal/mol by the rotation around the α axis, the energy change of CT is very little. The electron-density change, $\Delta\rho(r)$, in Table VI is similar to that of structure I.

In structure III $HCOO^-$ is rotated by 30° about the line parallel to the x axis through the position of O^{13} in $HCOO^-$ (β axis). One hydrogen bond is weakened in comparison with structure I. The difference of stabilization energy from

Table VII. Total Energies of Structure IV in Various Positions of $HCOO^-$ for Coordinate System of Structure I in Figure 2 (STO-3G Basis Set)

x axis, Å	y axis, Å	ΔE, kcal/mol
0.03726	-2.16000	-137.17
0.07726	-2.16000	-137.67
0.11726	-2.16000	-137.52
0.08795	-2.16000	-137.70
0.08795	-2.20000	-137.87
0.08795	-2.24000	-137.91
0.08795	-2.23225	-137.92

structure I is 20.3 kcal/mol. The decrease of the ES and CT terms contributes to this unstabilization. The CT term is due to $CT_{HCOO^- \rightarrow C(NH_2)_3^+}$. The coupling energy is due to COP_1. The electron-density changes of the part having one bending hydrogen bond are smaller than those of structure I.

Structure IV is obtained from the energy optimization as shown in Table VII. This structure, IV, corresponds to an ion pair of one hydrogen bond. As shown in Table II the difference of stabilization energy, 31.4 kcal/mol in comparison with structure I, is due to CT and ES. The electron-density change of H^6 is similar to that of structure I. On the other hand, electron density of H^9 almost does not change, since H^9 does not form a hydrogen bond. In the case of structures III and IV, the unstabilization occurs from the weakened hydrogen bond. Therefore, it was shown that the complex structure of the nearly parallel hydrogen bonds is very stable.

Structure V shows the rotated structure by 90° around the C^1–C^{11} line (γ axis) in structure I. The energy difference from structure I is 58.8 kcal/mol due to the large decrease of ES and CT terms (Table II). $CT_{HCOO^- \rightarrow C(NH_2)_3^+}$ was -12.9 kcal/mol, which was very small. The CT term was decomposed into four components: $CT_{\sigma-\sigma}$, $CT_{\pi-\sigma}$, $CT_{\sigma-\pi}$, and $CT_{\pi-\pi}$. $CT_{\sigma-\sigma}$ and $CT_{\pi-\sigma}$ were 63 and 37%, respectively. $CT_{\sigma-\pi}$ and $CT_{\pi-\pi}$ were almost zero. It is interesting that the contribution of $CT_{\pi-\sigma}$ is large.

Since the results of ab initio calculations for structure I are similar to those of the CNDO/2 method, the potential curves for the movement of $HCOO^-$ by using the CNDO/2 method were described in Figure 7. For movements of $-x$ and z direction, two hydrogen bonds are simultaneously broken, and, hence, potential energy becomes unstable with the increase of the distance from the origin. The potential curve of $-y$ direction has a local minimum, since one linear or bending hydrogen
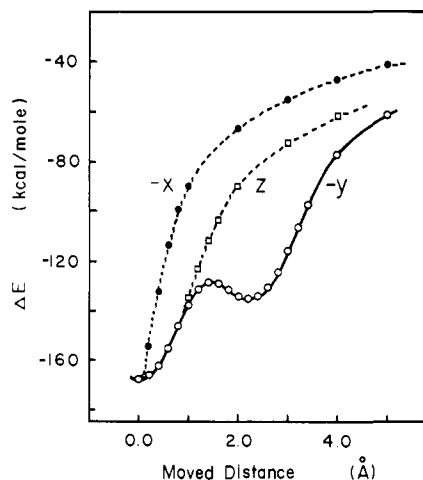
Figure 7. Potential curves of the complex between guanidinium ion and formic acid ion for movements of formic acid ion from the most stable structure by using the CNDO/2 method in kcal/mol. Molecular planes are shared by each other.

Figure 8. Potential curves of complexes between guanidinium ion and glycine zwitterion or glycine anion for distance between C^1 in guanidinium ion and C^{11} in glycine by using the CNDO/2 method in kcal/mol.

Table VIII. Total Interaction Energies between Guanidinium Ion and Glycine Zwitterion or Glycine Anion and Energy Decomposition Analyses in kcal/mol (STO-3G Basis Set)

	VI^a	VII	VII − VI
ΔE	−82.1	−168.8	−86.7
ES	−96.3	−157.1	−60.8
EX	101.9	96.7	−5.2
PL	−0.5	−8.0	−7.5
CT	−61.4	−71.5	−10.2
MIX	−25.8	−28.9	−3.1

^{a}Structures VI and VII are shown in Figure 3.

Table IX. Various Structures and Total Energies Obtained from Geometry Optimization for Complexes between Guanidinium Ion and Formamide in kcal/mol by Using the CNDO/2 Method

	$VIII^a$	IX	X	XI
ΔE	−25.5	−27.6	−28.5	−13.8

^{a}Structures VIII-XI are shown in Figure 4.

bond is reserved during the movement. Accordingly, it was shown that the reservation of one hydrogen bond is significant. This result is very useful when we consider movements of arginine residues in CPA.

Complex between Guanidinium Ion and Glycine. CPA produces an amino acid from the C-terminal of substrates by hydrolysis. A model of the product was calculated by using a complex of guanidinium ion and glycine zwitterion (structure VI in Figure 3). The complex of guanidinium ion and glycine anion as a model of the substrate was also calculated in comparison with the model of the product (structure VII in Figure 3). Table VIII shows the energy decomposition analyses of those structures. The terms obtained from structure VII are very similar to structure I. Therefore the substitution of –H by $-NH_2$ does not change the results of energy decomposition analyses. On the other hand, the terms obtained from structure VI were very different from structure VII. The protonation of $-NH_2$ of glycine unstabilized the interaction energy with guanidinium ion mainly due to the increase in the ES term as shown in Table VIII. Figure 6 shows the molecular orbital levels of glycine zwitterion and glycine anion. The MO levels of glycine anion almost do not change in comparison with the formic acid ion. However, the MO levels of the glycine zwitterion are lowered more than the glycine anion. Therefore, the stabilization by CT is smaller than that in structure VII. Since the changes of EX, PL, and MIX are relatively small, the electrostatic repulsion between the $-NH_3^+$ group in the glycine zwitterion and the guanidinium ion determines the unstabilization of structure VI. Figure 8 shows the potential curves of these complexes using the CNDO/2 method. The interaction force between the glycine anion and the guanidinium ion is larger than that between the glycine zwitterion and the gua-
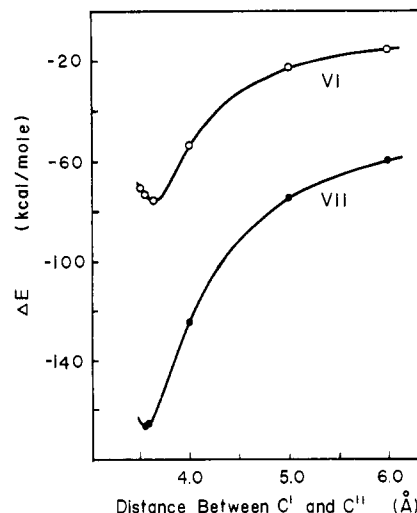
nidinium ion. Accordingly, after the hydrolysis of substrates by CPA, the interaction energy between Arg-145 and the amino acid product will be reduced largely.

Complex between Guanidinium Ion and Formamide. In CPA without substrate, Arg-145 interacts with the carbonyl oxygen of Gly-155. The second and third carbonyl oxygens of peptide backbones from the C-terminal of substrate are able to interact with Arg-127 and Arg-71, respectively. Therefore the calculations of four complex structures (VIII-XI) as shown in Figure 4 were carried out by using the CNDO/2 method. Structure VIII has a linear hydrogen bond. The hydrogen bond distance is 2.43 Å between N^5 and O^{11}. The angle ∠CON is 136.1°. Formamide and guanidinium ions lie on the same plane. IX and X show the bifurcated structures in which two $-NH_2$ groups of the guanidinium ion interact with the carbonyl oxygen. In structure IX two lone-pair orbits of the carbonyl oxygen participate in the interaction. In structure X π MO's on the carboxyl oxygen participate. After the energy optimization the distances between C^1 and O^{11} were 2.76 and 2.72 Å for structures IX and X, respectively. Structure XI shows the bifurcated structure in which a single $-NH_2$ group interacts with the carbonyl oxygen. The distance between N^2 and O^{11} after the energy optimization was 2.15 Å. Table IX shows the interaction energies for structures VIII-XI. Since IX and X were more stable, ab initio calculations for those structures were carried out by using the STO-3G basis set. In structure IX the distance between C^1 and O^{11} was optimized. The distance was 3.04 Å. For structure X the same distance as structure IX was used. The results are shown in Table X. IX was more stable than X by 3.0 kcal/mol. The decrease of stabilization energy was due to ES and CT. In order to elucidate the origin of CT, MO decomposition analysis was carried out. The CT term of IX is explained by the charge transfer between σ MO sets of both molecules. In structure X, 54.7% of the CT term comes from the MO interactions between the σ MO sets, and 45.2% is due to the MO interactions between the π MO
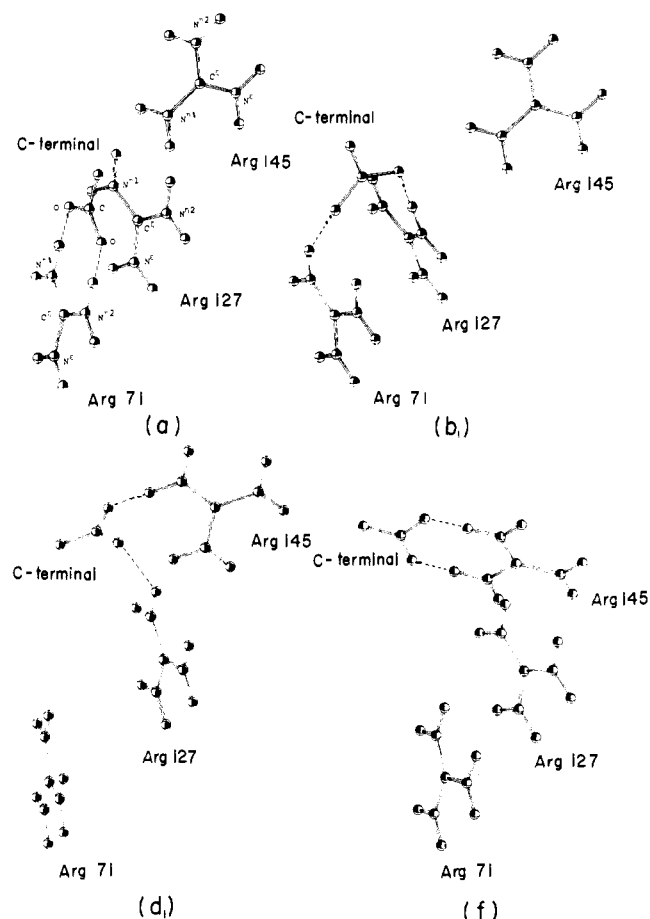
Figure 9. Figures showing the sliding system in which formic acid ion moves to Arg-145 through bindings with Arg-71 and Arg-127.
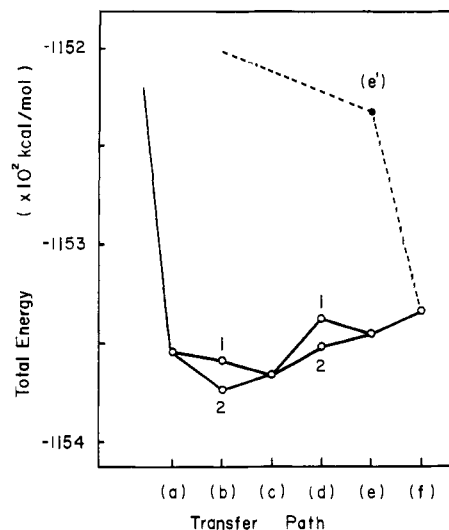

Figure 10. Potential curves of sliding of formic acid ion on three guanidyl groups of Arg-71, Arg-127, and Arg-145. The solid line is the potential curve in the sliding system. The broken line is a potential curve in the case where Arg-145 moves to the C-terminal carboxylate after the binding of substrate.

Table X. Total Interaction Energies and Energy Decomposition Analyses of Complexes IX and X between Guanidinium Ion and Formamide in kcal/mol (STO-3G Basis Set)

	IX[a]	X	X − IX
ΔE	−24.2	−21.2	3.0
ES	−22.8	−20.6	2.2
EX	19.4	18.0	−1.4
PL	−3.2	−3.4	−0.3
CT	−15.6	−13.9	1.7
MIX	−2.0	−1.2	0.8
CT_{B-A}[b]	−15.4	−13.2	2.2
$CT_{\sigma-\sigma}$	−15.4	−7.2	8.2
$CT_{\sigma-\pi}$		−0.0	
$CT_{\pi-\sigma}$		−5.9	

[a]Structures IX and X are shown in Figure 4. [b]A and B mean guanidinium ion and formamide, respectively.

set in the formamide and the σ MO set in the guanidinium ion. Accordingly, it was shown that contribution of the π MO set in formamide to the CT term increases largely as the structure changes from IX to X.

Sliding System. There are three arginine residues in the active-site groove of CPA. The guanidyl groups of Arg-71 and Arg-127 which were exposed to the surface of the enzyme may capture the C-terminal carboxylate of a substrate. During the catalytic step Arg-145 firmly binds with the C-terminal of the substrate in the active site. In crystallographic data of CPA, C^ζ atoms of Arg-71 and Arg-127 are separated by 4.7 Å, and those of Arg-127 and Arg-145 are separated by 6.4 Å. Since the distances among two arginines exposed to the surface of CPA and Arg-145 buried in the enzyme are near each other,

we assumed that the C-terminal carboxylate of the substrate may slide along three arginine residues before it fits to the final active site of Arg-145. Figure 9 shows some of calculated model structures. Table XI shows the movements from the coordinates of X-ray data. As an first recognition site of the substrate, Arg-71 may form an ion-pair structure involving two nearly parallel hydrogen bonds (model a in Figure 9). Then the C-terminal of the substrate may be transferred from Arg-71 to Arg-127, maintaining a hydrogen bond. Since the interaction-energy change between formic acid ion and guanidinium ion was relatively small in the $-y$ direction as shown in Figure 7, the conformation which conserves hydrogen bonds as much as possible should be considered as an intermediate state. Model b_1 in Figure 9 shows one intermediate model in which the C-terminal carboxylate of the substrate forms two hydrogen bonds, one with the guanidinium ion of Arg-71 and the other with Arg-127.[25] This interacting model is called the "bridge model". Again Arg-127 and the C-terminal carboxylate may form an ion-pair structure involving two hydrogen bonds as model a (model c). Model c is not shown in Figure 9. Next the bridge model between Arg-127 and Arg-145 may be formed as model d_1 in Figure 9. Again Arg-145 and the C-terminal carboxylate may form an ion pair involving two hydrogen bonds (model e). Model e is not shown in Figure 9. Finally the C-terminal carboxylate reaches the position obtained by the X-ray study. The C-terminal forms an ion-pair structure involving two nearly parallel hydrogen bonds with Arg-145, moving by about 2 Å from the initial position (Model f in Figure 9). The calculated result by the CNDO/2 method along the transfer path of the C-terminal is shown by a solid line in Figure 10. Since the energy differences between bridge models and two hydrogen-bond models are less than 20 kcal/mol, the C-terminal carboxylate is able to move smoothly and slide on the three arginines to the final goal in the active site. In addition, the transfer path of the substrate described in this paper is one of sliding models, and, hence, the transfer path with less energy differences will be obtained by more calculations. If Arg-145 moves to the C-terminal after the fitting of the substrate, the transfer path is represented by a potential curve shown with a broken line. In the calculated model the C-terminal carboxylate fits in the active site, and Arg-145 does not move, yet, toward the C-terminal (Model e'). The transfer path described by the solid line is more stable than that by the

Table XI. Rotations of Arg-71, Arg-127, and Arg-145 about Bonds of Arginine Residues for Each Model of Sliding System in C-terminal Transfer Process at Active Site of CPA

model	Arg-71			Arg-127			Arg-145			hydrogen bond N–H⋯O[b]
	C^β–C^γ	C^γ–C^δ	C^δ–N^ϵ	C^β–C^γ	C^γ–C^δ	C^δ–N^ϵ	C^β–C^γ	C^γ–C^δ	C^δ–N^ϵ	
a	0[a]	0	0	0	0	0	0	0	0	0
b₁	0	15	20	0	15	−25	0	0	0	90
b₂	0	−10	10	0	0	−30	0	0	0	90
c	0	0	0	0	0	0	0	0	0	0
d₁	0	0	0	0	−10	10	−10	40	0	90
d₂	0	0	0	0	−10	20	−10	30	10	70
e	0	0	0	0	0	0	0	0	0	0

[a]Unit is degrees. Original coordinates are obtained from the data by Lipscomb et al.[5c] Rotation is clockwise. [b]Rotation of C-terminal about a hydrogen bond, N–H⋯O, to clockwise direction.

Table XII. Effects of Neighboring Amino Acid Residues and Peptide Backbones on Movements from Model e to f of Arg-145 or Ion Pair between Arg-145 and C-Terminal Carboxylate in kcal/mol by Using the CNDO/2 Method

residue and peptide	(1)[a]	(2)[b]
Arg-71	1.0	3.1
Arg-127	−1.9	9.9
Asp-142	−2.7	−0.3
Asn-144	3.7	−16.4
Glu-163	4.3	−0.7
Thr-164	1.5	1.8
Tyr-248	0.0	1.5
Asp-246	−3.3	1.3
Asn-144–Arg-145	−1.9	0.0
Gly-155–Ala-156	14.2	6.0
Tyr-248–Gln-249	0.7	1.2
Gln-249–Ala-250	3.2	1.6
Ala-250–Ser-251	0.4	1.3
Gly-252–Gyl-253	1.6	1.6
the case where Tyr-248 was moved		
Tyr-248	−2.0	1.0
Tyr-248–Gln-249	2.1	0.9
Gln-249–Ala-250	2.7	1.2
Ala-250–Ser-251	−0.4	1.0

[a](1) means the movement of only Arg-145. [b](2) means the movement of the complex between Arg-145 and the C-terminal carboxylate.

broken line. This makes the sliding mechanism of the insertion of the C-terminal carboxyl group through the three arginine residues more reasonable.

Influence of Neighboring Residues on the Movement of Arg-145 in Carboxypeptidase A. The conformational changes in the active site of CPA, when Gly-Tyr binds, occur mainly in three amino acid residues, Arg-145, Glu-270, and Tyr-248. The guanidyl group of Arg-145 moves by about 2 Å from the initial position. The C-terminal carboxylate of the substrate forms a salt link with Arg-145. This motion of Arg-145 was necessary in order to fix the C-terminal of the substrate. However, this might be restricted by neighboring residues. In the sliding system the movement of the ion pair from model e to model f will be influenced by neighboring peptides. Effects of the neighboring residues, when Arg-145 or the ion pair is moved, are shown in Table XII. The interaction energy between Arg-145 and the peptide model of Gly-155-Ala-156 is reduced by 14 kcal/mol by the movement of Arg-145. Since the hydrogen covalently bonded to N^ϵ in the initial position of Arg-145 forms a hydrogen bond with the carbonyl oxygen of Gly-155,[5] Gly-155 has an effect on the motion of Arg-145. On the other hand, when Arg-145 and the C-terminal carboxylate maintaining the ion pair are moved together, the effects of the neighboring residues are shown in the second column. When

$N^{\delta 2}$ of Asn-144 forms a hydrogen bond with the carboxylate oxygen of the C-terminal, the stabilization energy of 16 kcal/mol is obtained. Arg-127 and Arg-71 which are located in the initial recognition site of the carboxylate group of the substrate have little influence. Since anion and cation charges are canceled on the ion pair, other neighboring residues do not influence largely. When the sliding model is considered, the results of the second column should be discussed. Since there are not the large positive values, the movement from model e to model f will occur smoothly without the interference of neighboring peptides. Moreover, the movements of Tyr-248 and the backbones do not interfere with the movement of the ion pair as shown in the Table XII.

Discussion

Jukes has proposed the hypothesis that relative scarcity of arginine in proteins is because arginine is a relatively new amino acid during the course of evolution.[26] However, since there appears to be no correlation between the rate of evolution and the lysine–arginine ratio, Wallis reported that the less frequency is attributed to a selection pressure against the occurrence of arginine, a role of arginine codons in control of protein synthesis, and the very high pK_a of arginine.[27] Riordan reported on the significance of arginyl residues as anion recognition sites in many enzymes.[2e] From the experiments of modification of CPA by butanedione, the loss of peptidase activity correlated nearly with the modification of three arginyl residues.[2b] Then the results of X-ray diffraction analyses showed that Arg-145 is a binding site for the C-terminal carboxylate group of the substrate.[5] There are Arg-71 and Arg-127 in the region of the binding groove away from the active center. In addition to Arg-145 which is the final recognition site of the carboxyl group, Arg-71 and Arg-127 might serve as an initial recognition site in the early stages of binding of substrates. It was shown in this paper from the enzyme dynamics that the C-terminal carboxylate group slides to Arg-145 with low potential barriers on the two arginyl residues, Arg-71 and Arg-127. The dynamical study of three arginines leads us to the sliding mechanism. After the binding of the C-terminal carboxylate to Arg-145, Arg-127 and Arg-71 are fitted to the carbonyl oxygens of the fourth and third amino acids, respectively, from the C-terminal of the substrate. After the C-terminal amino acid is hydrolyzed with the help of Glu-270, Tyr-248, and Zn^{2+}, etc., the newly produced C-terminal carboxylate is located in the active site. This carboxylate will be transferred to Arg-145. At the same time Arg-71 and Arg-127 will help the transfer of the substrate, sliding the C-terminal carboxylate group by ion-pair bindings. The experimental facts that modification of only two or three of the ten arginine residues of CPA reduces the peptide activity confirm the sliding mechanism.[2b] When CPA is modified by butanedione, it exhibits a K_m value for carbobenzoxyglycyl-

L-phenylalanine, identical with that of the native enzyme. Moreover, metal substitution at the active site profoundly affects the rate-determining step in the hydrolysis of peptides (k_{cat} values are in the order Co > Zn > Mn > Cd) but not their binding which is shown by K_m.[28] Therefore, elucidation of the binding process of the substrate at the active site is significant. By means of a three-component energy-transfer relay system, consisting of cobalt CPA, its fluorescent dansylated peptide substrates, and tryptophanyl residues of CPA, Latt et al. reported that distances between each dansyl peptide substrate and the cobalt CPA are in good agreement with those measured on Cory–Pauling–Koltun models from the center of the dansyl group of the extended peptides to the cobalt atoms interacting with the susceptible peptide carbonyl group.[29] When the catalysis and the distance from the active-site moiety to fluorescent substrate moieties of the enzyme–substrate complex were simultaneously measured, the increase in distance was a function of the extended chain length of peptides. When three arginyl residues were fitted to a substrate, the substrate must be extended in the binding groove. Then side-chain parts of the substrate approach to the hydrophobic part constructed by Phe-279 and Tyr-198, etc.

The determination of the crystal structure of the ternary complex of the staphylococcal nuclease with its inhibitor, thymidine 3′,5′-diphosphate, and calcium ion has revealed that the 5′-phosphate of the inhibitor forms two hydrogen bonds to each guanidyl group of Arg-35 and Arg-87.[3] Since a carboxyl group is very similar to a phosphate group with respect to their proton affinities[6d] and their structures, the structure also confirms the bridge model described in this paper. In lactate dehydrogenase Arg-101 interacts with the pyrophosphate group in coenzyme.[4] If positive and negative charges exchange with each other, the interacting structure is similar to the bridge model. And Arg-109 must pass through a ring composed of Asp-197, Asp-234, Asp-238, and Glu-107 during the conformational change between the apo and ternary complex structures.[4c] The case of CPA in which the C-terminal carboxyl group may slide over the three arginyl residues is very similar to that of lactate dehydrogenase, when carboxyl and guanidinium groups exchange with each other. The estimation of three essential arginines per subunit of lactate dehydrogenase from chemical modification studies by Yang and Schwert[2a] is confirmed by the indication of Arg-101, Arg-109, and Arg-171 located at the active site. The interaction between Arg-171 and L-lactate or pyruvate enol is the same as that between Arg-145 in CPA and the C-terminal carboxylate group of a substrate. The results of the interaction energies and the energy decomposition analyses are able to be applied to the interaction between Arg-171 in lactate dehydrogenase and L-lactate or pyruvate enol. The crystal structure of arginine glutamate monohydrate was determined in the studies on crystalline complexes among the amino acids.[30] The arginine and glutamate molecules have net positive and negative charges, respectively. The crystal structure contains a specific ion-pair interaction involving two nearly parallel N—H⋯O hydrogen bonds between the guanidyl group of arginine and the side-chain carboxylate group of glutamate. In the ab initio calculations for the ion-pair complex between guanidinium ion and formic acid ion, the most stable structure was determined: two parallel hydrogen-bond structures in which both molecules share the same plane. Though the complex of the C-terminal carboxyl group of Gly-Tyr and Arg-145 of CPA has two strong and weak bending hydrogen bonds in the coordinates reported by Lipscomb et al.,[5a] our calculations and the experiment by Bhat et al. predict that the complex between Arg-145 and the C-terminal carboxyl group has two parallel linear hydrogen bonds.

From the experimental fact that the arsanilazotyrosine-248·Zn complex of CPA is fully active in solution and that substrate binding disrupts the arsanilazotyrosine-248·Zn complex,[31] the movement of 12 Å of Tyr-248 was denied during the catalysis step. Moreover Lipscomb confirmed from the three-dimensional space-filling model that Tyr-248 is able to move to Zn^{2+} in the active enzyme.[32] After the movement of Tyr-248, therefore, the effects of the tyrosine residue and the backbone of peptides on the movement of the ion pair between the C-terminal carboxylate group and Arg-145 were calculated. Since Tyr-248 and backbones did not affect the movement of the ion pair, other mechanisms for the role of Tyr-248 should be considered.

Doscher and Richards demonstrated that, though kinetic parameters for ribonuclease S crystals were similar to those in solution, the former was not identical with the latter.[33] Harrison et al.[34] reported by stopped-flow techniques that the enzyme solution of CPA is an equilibrium mixture of at least three conformations. When the kinetic properties of the crystal were compared with those of solution, predominant effects on k_{cat} were observed. The k_{cat} in solution is 20–50 times larger than the k_{cat} in crystal for all esters and peptides. Moreover they indicated that X-ray crystallographic analyses may be unable to detect dynamic aspects of the enzymatic reaction, since the X-ray technique itself precludes them. Therefore, the dynamical study by moving Arg-71, Arg-127, and Arg-145 may be significant in order to elucidate the true enzymatic reaction in solution.

When CPA hydrolyzes a peptide from C-terminal, an amino acid is produced. The amino acid of the product has an $-NH_3^+$ and a $-COO^-$ group. The side-chain part is still in the pocket of the active site and the electronic structure changes from $-NHC<$ to $-NH_3^+$. Therefore the interaction energy between the isolated amino acid of the product and Arg-145 was calculated to compare with the interaction between the C-terminal amino acid and Arg-145. In order to simplify the calculations, $NH_2CH_2COO^-$ (glycine anion) and $NH_3^+CH_2COO^-$ (glycine zwitterion) were used in the place of the C-terminal amino acid of the substrate and the amino acid product, respectively. The interaction energy between glycine zwitterion and guanidinium ion was much less stable than the use of glycine anion by 61 kcal/mol. Therefore the C-terminal group salt linking with Arg-145 will easily leave the active site of the enzyme. After the hydrolysis, the new C-terminal carboxylate may interact with Arg-145 directly or by sliding after the interaction with Arg-71 or Arg-127. Auld and Holmquist reported that metal substitution at the active site of CPA changes the binding energy of esters (K_m^{-1} values in the order Co > Zn > Mn > Cd) but not their rate of hydrolysis.[28] They indicated that an interaction may occur between the metal atom and the carboxyl group of ester substrates. Riordan confirmed that ester substrate cannot bind with Arg-145,[2b] because butanedione modification of arginyl residues not only maintained esterase activity but also increased the activity to about 300% of the control. The product of ester substrate is an anionic structure since ester activity is generally determined by titration of the protons released on hydrolysis. Therefore, the negatively charged product binding with Arg-145 will not leave easily when the ester substrate is hydrolyzed in the same reaction path as the amide substrate. Accordingly, one of the reasons why Arg-145 does not interact with the carboxyl group of the ester substrate may be attributed to the difficulty of its leaving Arg-145 site.

References and Notes

(1) Presented in part before the 16th Annual Meeting of the Japanese Biophysics Society, Sendai, Sept 1977.

(2) (a) P. C. Yang and G. W. Schwert, *Biochemistry*, **11**, 2218 (1972); (b) J. F. Riordan, *ibid.*, **12**, 3915 (1973); (c) C. L. Borders, Jr., and J. F. Riordan, *ibid.*, **14**, 4699 (1975); (d) L. Patthy and E. L. Smith, *J. Biol. Chem.*, **250**, 565 (1975); (e) J. F. Riordan, K. D. Mcelvany, and C. L. Borders, Jr., *Science*, **195**, 884 (1977).

(3) (a) F. A. Cotton and E. E. Hazen, Jr., "The Enzymes", Vol. IV, P. D. Boyer, Ed., Academic Press, New York, N.Y., 1971, Chapter 7; (b) A. Arnone, C. J. Bier, F. A. Cotton, V. W. Day, E. E. Hazen, Jr., D. C. Richardson, J. S. Richardson, and A. Yonath, *J. Biol. Chem.*, **246**, 2302 (1971); (c) F. A. Cotton, V. W. Day, E. E. Hazen, Jr., S. Larsen, and S. T. K. Wong, *J. Am. Chem. Soc.*, **96**, 4471 (1974).

(4) (a) M. J. Adams, M. Buehner, K. Chandrasekhar, G. C. Ford, M. L. Hackert, A. Liljas, M. G. Rossmann, I. E. Smiley, W. S. Allison, J. Everse, N. O. Kaplan, and S. S. Taylor, *Proc. Natl. Acad. Sci. U.S.A.*, **70**, 1968 (1973); (b) J. J. Holbrook, A. Liljas, S. J. Steindel, and M. G. Rossmann, "The Enzymes", Vol. XI, P. D. Boyer, Ed., Academic Press, New York, N.Y., 1975, Chapter 4; (c) W. Eventoff, M. G. Rossmann, S. S. Taylor, H.-J. Torff, H. Meyer, W. Keil, and H.-H. Kiltz, *Proc. Natl. Acad. Sci. U.S.A.*, **74**, 2677 (1977).

(5) (a) W. N. Lipscomb, J. A. Hartsuck, G. N. Reeke, F. A. Quiocho, P. H. Bethge, M. L. Ludwig, T. A. Steitz, H. Muirhead, and J. C. Coppola, *Brookhaven Symp. Biol.*, **21**, 24 (1968); (b) W. N. Lipscomb, G. N. Reeke, Jr., J. A. Hartsuck, F. A. Quiocho, and P. H. Bethge, *Philos. Trans. R. Soc. London, Ser. B*, **257**, 177 (1970); (c) F. A. Quiocho and W. N. Lipscomb, *Adv. Protein Chem.*, **25**, 1 (1971); (d) W. N. Lipscomb, paper presented at The Robert A. Welch Foundation Conferences on Chemical Research, XVth, 1971, Bio-Organic Chemistry and Mechanisms.

(6) (a) H. Umeyama, A. Imamura, C. Nagata, and M. Hanano, *J. Theor. Biol.*, **41**, 485 (1973); (b) H. Umeyama, *Chem. Pharm. Bull.*, **22**, 2518 (1974); (c) H. Umeyama, A. Imamura, and C. Nagata, *ibid.*, **23**, 3045 (1975); (d) H. Umeyama, presented in part at the 28th Annual Meeting of Japanese Protein Structure, Tokyo, Oct 1977.

(7) S. Nakagawa and H. Umeyama, *Chem. Pharm. Bull.*, **25**, 909 (1977).

(8) H. Umeyama, A. Imamura, C. Nagata, and S. Nakagawa, *Chem. Pharm. Bull.*, **25**, 1685 (1977).

(9) (a) R. Hoffmann and W. N. Lipscomb, *J. Chem. Phys.*, **37**, 2872 (1962); (b) S. Scheiner and W. N. Lipscomb, *J. Am. Chem. Soc.*, **99**, 3466 (1977).

(10) D. M. Hayes and P. A. Kollman, *J. Am. Chem. Soc.*, **98**, 7811 (1976).

(11) J. A. Pople and G. A. Segal, *J. Chem. Phys.*, **44**, 3289 (1966).

(12) W. J. Hehre, W. A. Lathan, R. Ditchfield, M. D. Newton, and J. A. Pople, GAUSSIAN 70, Program 236, Quantum Chemistry Program Exchange, Indiana University, 1973.

(13) C. K. Johnson, ORNL-3794 Oak Ridge National Laboratory, Oak Ridge, Tenn., 1971.

(14) (a) K. Morokuma, *J. Chem. Phys.*, **55**, 1236 (1971); (b) S. Yamabe and K. Morokuma, *J. Am. Chem. Soc.*, **97**, 4458 (1975); (c) K. Kitaura and K. Morokuma, *Int. J. Quantum Chem.*, **10**, 325, (1976).

(15) (a) H. Umeyama, K. Kitaura, and K. Morokuma, *Chem. Phys. Lett.*, **36**, 11 (1975); (b) H. Umeyama and K. Morokuma, *J. Am. Chem. Soc.*, **98**, 4400 (1976); (c) *ibid.*, **98**, 7208 (1976); (d) H. Umeyama and S. Nakagawa, *Chem.*

(16) S. Nagase, T. Fueno, S. Yamabe, and K. Kitaura, *Theor. Chim. Acta*, in press.

(17) H. Umeyama and T. Matsuzaki, *Proc. Int. Congr. Pure Appl. Chem.*, *26th*, 309 (1977).

(18) L. E. Sutton, "Tables of Interatomic Distances and Configurations in Molecules and Ions", *Chem. Soc.*, *Spec. Publ.*, *Suppl.*, **No. 18** (1965).

(19) P.-G. Jonsson and A. Kvick, *Acta Crystallogr.*, *Sect. B*, **28**, 1827 (1972).

(20) T. Nishikawa, *J. Phys. Soc. Jpn.*, **12**, 668 (1957).

(21) Though the coordinates of the complex of Arg-145 and C-terminal carboxylate were reported in 1968, they were incredible to be used for MO calculations. Therefore, we used the coordinates reported in 1971 by Lipscomb et al.[5] However, the latter paper did not show the complex coordinates.

(22) Since this result was obtained from the STO-3G basis set, the dependence of the basis set must be considered. In comparison with the calculations by using the 4-31G basis set of double ζ level, the results of STO-3G calculations overestimate CT. In consideration of the basis set dependency, the fact that CT is smaller than ES shows the importance of the ES term.

(23) The charge-transfer energy 72.4 kcal/mol is very large. The value is explained in relation to distance, 1.357 Å, between H in $C(NH_2)_3{}^+$ and O in $HCOO^-$. This is very short in comparison with those of hydrogen bonds between two neutral molecules.[24] Therefore, the large interatomic overlaps of H and O, in addition to the differences between intermolecular orbital levels, may contribute to the CT value.

(24) H. Umeyama and K. Morokuma, *J. Am. Chem. Soc.*, **99**, 1316 (1977).

(25) An oxygen of C-terminal carboxylate forms a hydrogen bond as shown by structure III in Figure 2. Another oxygen forms a hydrogen bond with a distance between oxygen and hydrogen in arginine of 1.738 Å. This structure is described as model b_1. Moreover, in the case where the distance of the latter hydrogen bond is shortened to 1.328 Å, the structure is shown as model b_2. In order to avoid artificial results, therefore, two models, b_1 and b_2, were considered. Two models, d_1 and d_2 are similar to those of b_1 and b_2, and the distances of bending hydrogen bonds are 1.997 and 1.379 Å, respectively. Bending hydrogen bonds occur to keep van der Waals distance between the $-NH_2$ group and the carbon of the C-terminal carboxyl. Distances between Arg-71 and Arg-127 and between Arg-127 and Arg-145 are over van der Waals contact.

(26) T. H. Jukes, *Biochem. Biophys. Res. Commun.*, **53**, 709 (1973).

(27) M. Wallis, *Biochem. Biophys. Res. Commun.*, **56**, 711 (1974).

(28) D. S. Auld and B. Holmquist, *Biochemistry*, **13**, 4355 (1974).

(29) S. A. Latt, D. S. Auld, and B. L. Vallee, *Proc. Natl. Acad. Sci. U.S.A.*, **67**, 1383 (1970).

(30) T. N. Bhat and M. Vijayan, *Acta Crystallogr.*, *Sect. A*, **31**, S48 (1975).

(31) (a) F. A. Quiocho, C. H. Mcmurray, and W. N. Lipscomb, *Proc. Natl. Acad. Sci. U.S.A.*, **69**, 2850 (1972); (b) J. T. Johansen and B. L. Vallee, *ibid.*, **70**, 2006 (1973); (c) L. W. Harrison, D. S. Auld, and B. L. Vallee, *ibid.*, **72**, 3930 (1975); (d) C. A. Spilburg, J. L. Bethune, and B. L. Vallee, *Biochemistry*, **16**, 1142 (1977).

(32) W. N. Lipscomb, *Proc. Natl. Acad. Sci. U.S.A.*, **70**, 3797 (1973).

(33) M. S. Doscher and F. M. Richards, *J. Biol. Chem.*, **238**, 2399 (1963).

(34) L. W. Harrison, D. S. Auld, and B. L. Vallee, *Proc. Natl. Acad. Sci. U.S.A.*, **72**, 4356 (1975).